Acoustic Mode Measurements in the Inlet of a Turbofan Engine

P. D. Joppa*
The Boeing Commercial Airplane Company, Seattle, Washington

Turbomachinery noise propagates in aircraft jet engine ducts in a complicated manner. The measurement of this propagation is useful both to identify source mechanisms and to design efficient linings. A practical method of making these measurements has been developed using linear arrays of equally spaced microphones mounted flush with the duct wall. Circumferential or axial arrays are analyzed by spatial Fourier transform, giving the sound level as a function of the spinning order or axial wavenumber, respectively. Complex demodulation is used to acquire data in a modest bandwidth around a high frequency of interest. A joint NASA/Boeing test of the system used 32 microphones in a JT15D turbofan engine inlet. A 400-Hz bandwidth centered at blade passage frequency and at one-half blade passage frequency was studied. The theoretically predicted modes were clearly seen at blade passage frequency; broadband noise at one-half blade passage frequency was biased toward modes corotating with the fan. Interference between similar modes was not a significant problem. A lining design study indicated that a 15% improvement in lining efficiency was possible for this particular engine when mode data were used. The technique has proved reliable and useful for source diagnostics and lining design.

Introduction

NOISE from commercial aircraft operations continues to be a source of community annoyance. A significant portion of this noise is generated within the engines by the fan and compressor unit. The resulting noise propagates through the inlet and exhaust ducts in a complicated manner, eventually radiating from the engine to the ground. This noise can be either reduced at the source or attenuated by the use of sound-absorbent linings in the ducts. Identifying the source mechanisms or designing optimal linings requires some knowledge of just how the noise is propagated through the ducts. Making measurements of this propagation is the subject of this paper.

The usual approach to duct acoustics problems is to approximate the duct by an infinite cylinder in a separable coordinate system (e.g., a circular or annular cylinder) and solve the differential equations by separation of variables. This leads to an eigenvalue problem, the solutions of which are the duct propagation modes. Each mode represents a different way in which sound may travel down the duct; for typical turbofan engines at blade passage frequencies there may be several hundred such modes. A complete description of the sound field in the duct consists of knowing the complex amplitude of each mode. Because the optimum sound-absorbing lining is different for each mode, knowledge of the relative modal amplitudes is highly desirable for lining design. In addition, the various source mechanisms will each excite different sets of modes, so that a knowledge of the modal amplitudes can help isolate the cause of a noise problem.

The method selected here for mode measurement involves a large number of microphones flush-mounted on the inside surface of the duct. This is not ideal in terms of identifying the modes, but it avoids wake-producing objects inserted into the flow.

To understand why this should be avoided, we must describe the acoustic modes in a little more detail. No attempt is made here to derive the separation-of-variables solution to the wave equation in a duct; for a more rigorous treatment, see Ref. 1. The geometry is shown in Fig. 1. For a cylindrical duct, the solution is written as

$$p(r,\theta,z,t) = \sum_{m,n} A_{mn} \exp[i(m\theta + k_z z - \omega t)] J_m(k_{mn} r)$$

where r,θ,z are the cylindrical coordinates, t the time, p the acoustic pressure, J_m the Bessel function of order m, k_{mn} the eigenvalue of the (m,n)th mode, and k_z the axial component of the wave vector. Qualitatively, each mode (of amplitude A_{mn}) has a characteristic shape in a cross section of the duct $[e^{im\theta} J_m(k_{mn} r)]$ which propagates down the duct.

Clearly then, the easiest way to identify a mode in a duct is to measure the acoustic pressure distribution over a cross section of the duct. Unfortunately, this measurement involves putting a microphone into the flow. In fact, as will be seen later, many microphones must be used. These microphones, in the inlet duct for example, will have wakes whose interaction with the fan rotor might generate noise louder than the fan noise to be measured. An alternative, nonintrusive mode measurement approach would eliminate this problem.

The clue is found in the nature of the wave equation solution. Propagation in the three coordinate directions (axial, radial, and circumferential) is not independent. The radial propagation can be calculated from the axial and circumferential propagation measurements—both of which can be made on the duct surface.

Analysis

There are two basic approaches to characterizing the sound field in a duct from surface acoustic pressures. If there are few modes (relative to the number of pressure measurements), then the individual modes can in theory be identified. When there are very many modes, they must be characterized as a distribution, with respect to wavenumber, for example. Both of these methods have been applied to duct mode measurements in the past.[2,3]

The analysis for a small number of modes is very appealing. Because almost all duct acoustics are done in terms of modes, it is highly desirable to know the individual modal amplitudes. If there are fewer modes than microphones, a simple least-squares fit will provide the modal amplitudes, and the microphone locations are not constrained. Even at high frequencies, where many modes can propagate, this method

Presented as Paper 84-2337 at the AIAA/NASA 9th Aeroacoustics Conference, Williamsburg, VA, 1984; received June 22, 1986; revision received Feb. 13, 1987.

*Senior Specialist Engineer. Member AIAA.

should work if most of the modes occur at a sufficiently low level, with only a few at a high level.

The main problem with this approach lies with the least-squares algorithm. In general, if any of the modes are very similar to each other, then the numerical problem has poor stability. This means that the acoustic pressures must be known to high accuracy, and there must be very little contamination from the modes that are ignored. The range of application of this approach can be extended somewhat by choosing microphone locations that maximize the numerical stability, but the fundamental limitation remains.

The other approach to mode measurement, and the one chosen here, is to regard the sound field as a continuous distribution of energy with wavenumber, instead of as a set of discrete modes. This method works particularly well for cases with a very large number of modes because similar modes are grouped together, so no attempt is made to identify them separately. Thus, the numerical methods are stable and robust (insensitive to small calibration errors and other data contamination). The corresponding disadvantage is that modes grouped together may cancel or reinforce each other; the method would work best with a truly continuous distribution of modes. In cases where the modes are well separated, the two approaches can give similar results.

The wavenumber distribution method is implemented with an equally spaced linear array of microphones disposed along an axis of the (cylindrical) duct coordinate system (see Fig. 1). This will give, by discrete Fourier transform, a spectrum of sound pressure level (SPL) vs the component of the wave vector in that coordinate. For instance, an axial array gives SPL as a function of the axial wavenumber; a circumferential array gives SPL vs the circumferential wavenumber, usually interpreted as the spinning order. While the radial/circumferential description would be convenient mathematically because it describes the "characteristic shape" feature of the modes, the axial/circumferential pair has useful practical meanings. The axial speed of a mode determines its "residence time" in a particular length duct; this is a very important parameter for lining design and performance estimation.[4] The circumferential (spinning order) distribution is closely related to fan noise source mechanisms. Both of these arrays can be surface-mounted so they do not disturb the noise source mechanisms.

This approach is limited in accuracy by the number of microphones available. The microphones must be close together to avoid aliasing, but the resolution is inversely proportional to the total array length. Sparse arrays have been used in underwater acoustics to improve resolution without increasing the number of sensors, but they rely on the various signals being uncorrelated, so that the field is spatially stationary.[5] This is unfortunately not true of duct noise, where several modes come from the same source and are thus highly correlated. Random arrays (which are free of aliasing) have poor signal-to-noise ratios unless they are very large—hundreds or thousands of microphones would be needed for satisfactory duct acoustics measurements.

Data Acquisition

The modal structure in an engine duct is clearly a function of frequency—sounds at different frequencies are generated by different mechanisms and couple into the various modes differently. Thus, to do modal analysis, we need the microphone pressures as complex numbers at the frequency of interest. In addition to single frequencies, such as the blade passage frequency tone, we are interested in broadband noise and unsteady tones. What is really needed, then, is the complex pressure in a band of frequencies. If it is sampled rapidly enough to avoid aliasing, all the information will be retained and arbitrary further analyses will be possible.

Signal averaging, which is often used to extract the complex amplitude of a tone in the presence of noise, is unsatisfactory because it has a very narrow equivalent bandwidth. Even tone data, if the tone is unsteady, can be misestimated with this

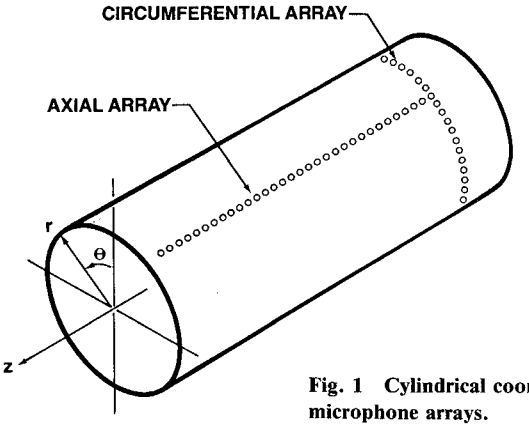

Fig. 1 Cylindrical coordinates and microphone arrays.

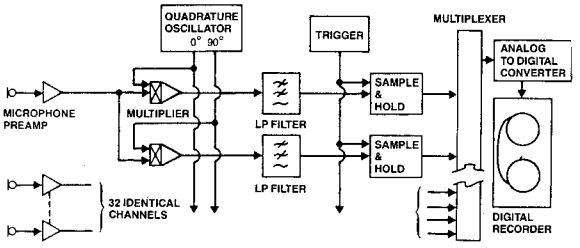

Fig. 2 Data preprocessor for modal analysis.

technique. At the other extreme, the ideal solution would be to sample each microphone very rapidly and use a fast Fourier transform (FFT) analysis to calculate the complex pressure as a function of frequency over the whole spectrum. This is not very practical, however, because it requires a real-time FFT analyzer for each microphone and generates enormous amounts of data.

A "zoom FFT" (sometimes called quadrature demodulation) could reduce the amount of data by using only a specified band out of the whole spectrum. The method chosen here emulates that process with an analog zoom followed by digital recording. The signal from each microphone is multiplied both in phase and 90 deg out of phase with a fixed-frequency signal in the frequency band under investigation. The result is a complex pair of signals, frequency-shifted so that the fixed frequency is now zero Hz. These signals are low-pass filtered to select out the components near zero Hz, which are the components of the original microphone signal near the fixed frequency. In the present instance, low-pass filters with a 200-Hz cutoff are used, so information is obtained from a band of frequencies of ±200 Hz around the fixed frequency. These complex low-frequency signals are sampled above the Nyquist rate of twice the maximum frequency—a 500-Hz sample rate is used here to provide some margin—and recorded in digital form for later analysis. A block diagram of the system is shown in Fig. 2.

This system is calibrated in three ways—the electronics (primarily the low-pass filters) are calibrated for dc drift and frequency response, and the microphones are calibrated for frequency response. All the calibrations are relative calibrations, arbitrarily referred to channel 1. The electronics calibration is conventional, using shorted inputs for drift and white noise inputs for frequency response. The microphone calibration, however, is a new process developed to calibrate all the microphones at once. The microphones are flush-mounted in a narrow tube of 12.7-mm-square cross section, with a loudspeaker driver at one end and an anechoic termination at the other (see Fig. 3). By exchanging the driver and termination, enough information can be obtained to calculate the microphone calibrations, the wave amplitudes including the

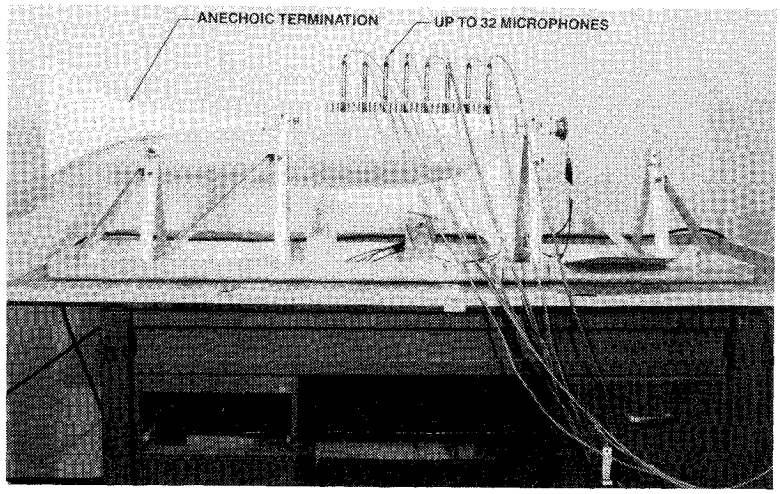

Fig. 3 Microphone calibration duct.

small reflected wave, the wave speed, and the tube attenuation. This problem is nonlinear but can be linearized. It is solved by iteratively applying a least-squares solution of the linearized problem. Accuracies of about 0.1-dB amplitude and 1-deg phase, compared with pistonphone and electrostatic actuator calibrations, have been obtained with 6.35-mm condenser microphones.

Experimental Results

The system as previously described, was developed over several years of testing with mode generators and model-scale fan rigs. It was recently tested on a full-scale jet engine, the JT15D, in a joint experiment conducted by NASA and Boeing. NASA provided the engine, test stand, special inlet hardware, and test crew while Boeing provided the mode measurement system, the microphones, and the data analysis. The test was conducted in November 1982 on a taxiway and runup ramp at NASA's Langley Research Center. The test layout is shown in Figs. 4 and 5 (the OV-1 aircraft was functioning as a data van for this test). Figure 6 is a closer view of the engine, extension duct, and inflow control device (ICD).

The test engine, a modified JT15D turbofan, is a twin-spool, front-fan engine with a full-length bypass duct. It has a nominal bypass ratio of 3.3 and a maximum thrust capability of 9786 N (see Fig. 7 for specifications).

The 0.533-m-diam fan has 28 blades (see Fig. 8). The fan is followed by a stator assembly consisting of a bypass stator with 66 vanes and a core stator with 71 vanes. The latter is the only major difference between a production JT15D engine (which has 33 core-stator vanes) and the test engine. The modified core stator has more blades and is aft of the rotor blade root a distance of 0.63 fan-blade root chord (compared with 0.28 chord for a production engine) in order to acoustically cut off the fan-rotor/core-stator interaction tone and diminish the broadband noise. The next rotating blade assembly is the compressor, which is a combination axial-centrifugal compressor having 16 blades in the leading axial part of the unit.

As shown in Fig. 8, the engine core is supported by six internal struts that are located in the intermediate case of the engine. These supports traverse the compressor and bypass ducts to attach the core to the outer wall of the engine intermediate case. These struts are located downstream of the stator assembly.

Mode measurements were made in a cylindrical extension duct, 1.824 m long, mounted between the fan case and the ICD, shown in Fig. 9. Microphones are visible in Fig. 9, mounted in a half-circle circumferential array. This microphone spacing, 1/64 of the circumference, permits spinning orders up to ± 32 to be detected without aliasing. The axial array at the bottom of the duct holds the 32 microphones

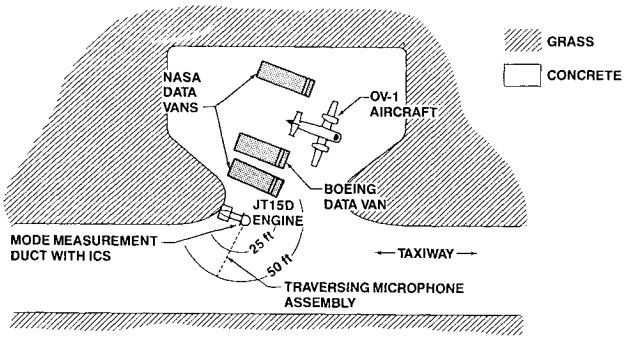

Fig. 4 Test layout.

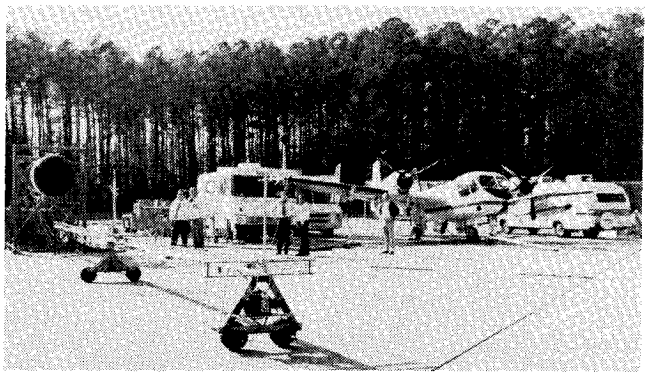

Fig. 5 Test arena.

spaced 50.8 mm apart. At frequencies above about 3 kHz, this spacing would cause some aliasing, because the Nyquist limit requires that the microphones be less than one-half wavelength apart. Up to about 6.5 kHz, however, the aliased waves show up as backward-going waves. Because previous model-scale tests had confirmed the absence of such waves, the aliased data can be reinterpreted as forward-going and a substantial increase in resolution obtained. Static pressure taps are located approximately every 76 mm along the duct. The duct extension could be rotated about its axis and clamped in any position. The modal data system used 32 6.35-mm condenser microphones. The zoom bandwidth recorded was about 400 Hz, centered at blade passage frequency and at one-half blade passage frequency, with a sample rate of 500 Hz. The microphones were calibrated in the morning and evening of each test day.

Slightly over two minutes of data were recorded at each condition. The pressure data were analyzed with a Hanning-windowed FFT, ensemble averaged for about 4 s; a total of 32

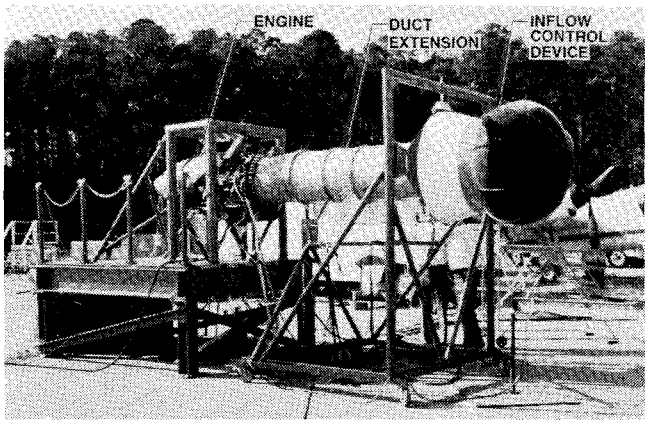

Fig. 6 Engine installation.

ITEMS	VALUES
FAN SPEED (MAX), r/min	16,000
FAN PRESSURE RATIO	1.5
BYPASS RATIO (MAX)	3.3
ROTOR BLADES	28
ROTOR DIAMETER, m	0.533
HUB/TIP RATIO	0.405
BYPASS-STATOR VANES	66
CORE-STATOR VANES	71[a]
ROTOR/BYPASS-STATOR SPACING	1.83
ROTOR/CORE-STATOR SPACING	0.63[b]
COMPRESSOR SPEED (MAX), r/min	32,760
CORE EXHAUST AREA, m^2	0.051
BYPASS EXHAUST AREA, m^2	0.092

[a]PRODUCTION ENGINE HAS 33 CORE-STATOR VANES

[b]PRODUCTION ENGINE CORE-STATOR SPACING IS 0.28, NORMALIZED TO FAN-BLADE ROOT CHORD

Fig. 7 JT15D specifications.

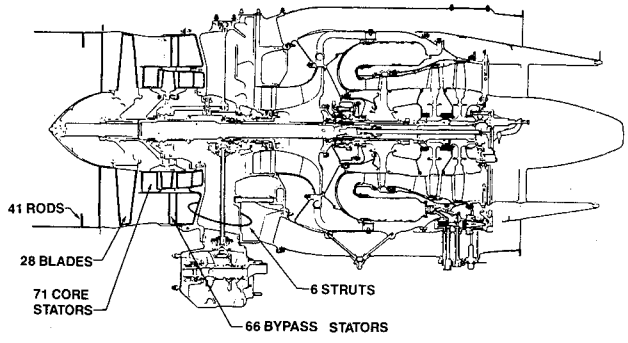

Fig. 8 JT15D engine.

wavenumber spectra were obtained from each condition. These spectra, plotted together, give some indication of the unsteadiness of the sound field. The spectra are plotted as a function of the spinning order for the circumferential-array data or the axial wavenumber in m^{-1} for the axial array.

The modal data indicate, for the most part, the existence of the expected modes and no others. A major interesting feature is the strong presence of the rotor/strut interaction mode. This mode would not normally have been expected, but earlier blade-mounted transducer data had suggested its existence, at least as a pressure field.[6]

Before looking at mode plots, a discussion of the expected modes at blade passage frequency (BPF) is in order. Rotor/stator interactions are cut off (i.e., the mode order is too high for it to propagate in the duct) and thus are not expected (28 blades interacting with 66 stators and 71 core stators would produce spinning orders of $m = -38$ and -43, according to the usual Tyler-Sofrin theory).[7] Rods were installed in front of the fan to generate a strong propagating mode (41 rods give $m = -13$). Up to three radial orders of the -13 spinning order can propagate in the duct. The six downstream struts will generate the $m = 22$ spinning order. For supersonic tip speeds, the $m = 28$ rotor-alone field can propagate also.

The cut-on points of the various modes are shown in Fig. 10 as a function of engine speed. Note that the target speeds were chosen to be between the cut-on points of the first few modes expected, so that each speed would have one more mode cut on than the previous one.

The circumferential modal distributions at blade passage frequency are shown in Fig. 11 for all the speeds. At 6200 r/min, with the rods installed, broadband noise is seen within the range of spinning orders that are cut on ($m = \pm 12$). At 8000 r/min, the $m = -13$ rod interaction mode has become cut on and remains present at all the higher speeds. By 10,450 r/min, the strut interaction mode $m = 22$ has also appeared. It remains at 10,800 r/min but has disappeared by 13,500 r/min. This mode is presumably generated downstream of the fan blade leading edges and thus cannot propagate through the shock waves (the fan tip relative Mach number is 1.0 at approximately 11,600 r/min). The rotor-locked field, $m = 28$, is present only at 13,500 r/min, as expected. Note that this mode is steadier in level than the others. Figure 11 shows similar data with the rods removed at 9600 and 10,800 r/min; note the disappearance of the $m = -13$ mode.

The axial wavenumber spectra corresponding to Fig. 11 are shown in Fig. 12. Note the single mode at 8000 r/min (with the rods) and the two modes at 9600 r/min. Since only the $m = -13$ spinning order is present, these must be the first and second radial orders. At 10,450, the third radial of $m = -13$ appears, along with the $m = 22$ mode (first radial). This speed was chosen to be just below the cut-on of the $m = 22$ strut in-

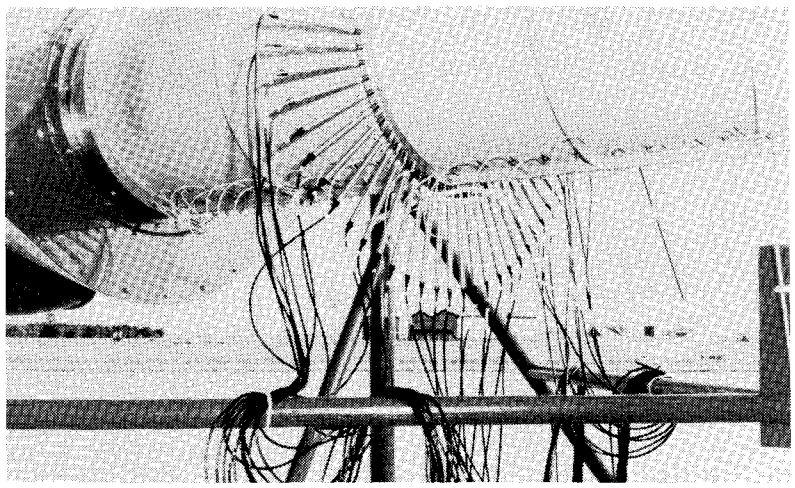

Fig. 9 Inlet extension duct with circumferential microphone array.

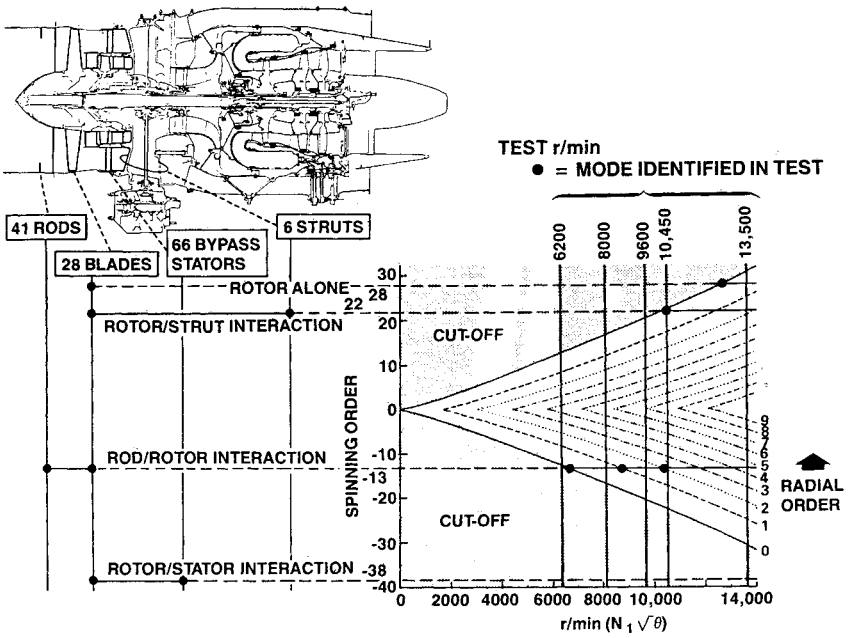

Fig. 10 Expected modes in the inlet of JT15D engine.

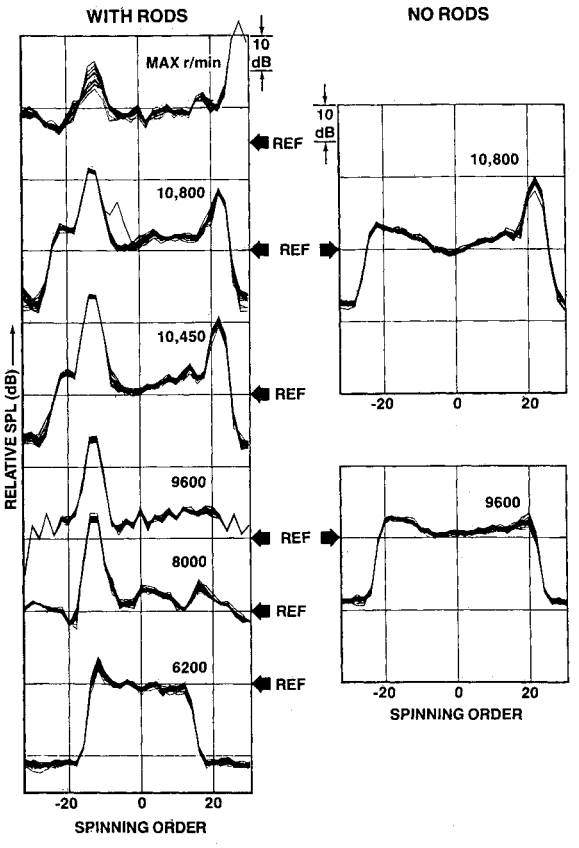

Fig. 11 SPL vs spinning order at blade passage frequency.

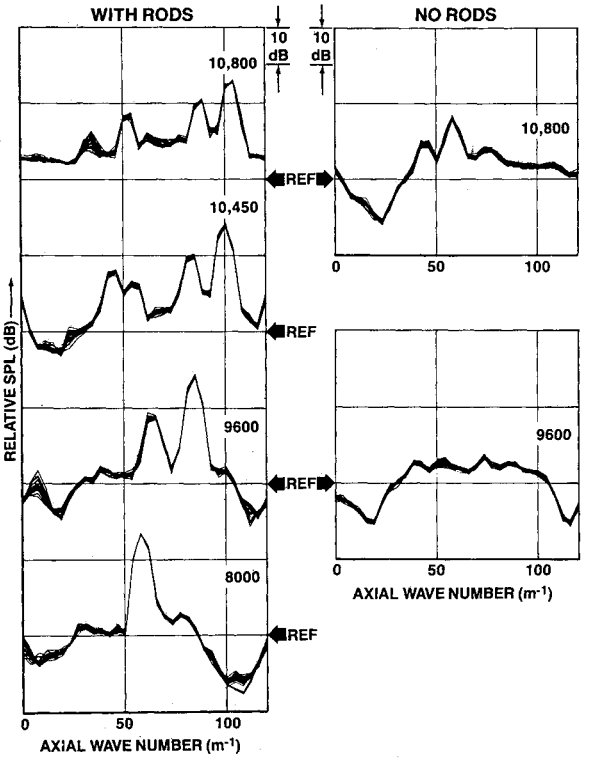

Fig. 12 SPL vs axial wavenumber at blade passage frequency.

teraction, but the mode was present because the actual speed was a little high. The data at 10,800 r/min are very similar; no BPF data were taken with this array at maximum r/min. The no-rod data show, as expected, no modes at 9600 r/min. At 10,800 r/min, the plot seems a little peculiar. The dominant mode has a wavenumber slightly too high (this may be due to a higher speed than targeted), and the background noise is high except at low wavenumbers (this may be a sign of the failure of one or more microphones during the test). The main features of the plot are as expected, but the high background noise level makes it difficult to be certain that there is only one mode. The circumferential data, however, indicate only the $m = 22$ order, and only one radial order of that mode will propagate at this speed.

The spinning order data at one-half BPF are shown in Fig. 13. At maximum r/min, with buzzsaw noise being generated, all the energy is expected to be in the $m = +14$ mode (half of the 28 blades). No explanation is offered for the apparent presence of an $m = -14$ mode. At lower speeds, the features are a broadband modal structure within the range of propagating modes, biased toward the corotating modes. The small spikes near $m = +10$ at 10,450 and 10,800 r/min may possibly be an $m = +11$ mode, generated by the nonlinear propagation of the $m = 22$ BPF mode that is just cut on, the so-called subsonic buzzsaw effect.

One of the potential problems with this method of mode measurement is that the modal structure is measured at a single location. A single FFT bin of the wavenumber spectrum may include several modes. Depending on their phases, these modes may cancel or reinforce each other at a particular array position. To get a more accurate modal spectrum, the technique of ensemble averaging could be used—averaging the spectrum over many positions of the array. To test the significance of this, the same axial measurement was repeated at different rotation angles of the duct (see Fig. 14). Generally, these plots show the same features, with small variations in the relative amplitudes of the various modes. At least for this engine, modal interference does not appear to be a severe problem.

Impact on Lining Design

Normally, lining designs are optimized assuming that acoustic energy is evenly distributed among all the propagating modes. The resulting design is close to optimum for only a few modes, which might be called "typical" modes; such a lining design is far from optimum for most modes. With mode measurement, however, it is always possible to find an optimum lining design. It would be expected to perform significantly better in most cases than the uniform-distribution lining design.

To illustrate this, hypothetical linings were designed for the JT15D. Two linings were designed, one for a uniform modal distribution and one for the observed JT15D modes, with the rods installed. Each lining was chosen to be a compromise for the three engine speeds, 8000, 9600, and 10,450 r/min. These engine speeds and the inclusion of the rods were chosen to match both the mode measurement test and a lining flight test.[8] The duct parameters, also chosen to match Ref. 8, are shown in Fig. 15a. The linings were chosen to be double-layer types with two honeycomb cores and two purely resistive screens as shown in the sketch, Fig. 15b.

The observed modal distributions for the chosen conditions are shown in Fig. 15c. Note that the $m = -13$ spinning order modes dominate; the $m = 22$ mode is present in only one case, and at a low level. Since the $m = 22$ is also close to cutoff and thus easily attenuated by any lining, it was ignored. The two linings were designed and evaluated assuming either a uniform distribution among all spinning modes or just the $m = -13$ spinning order modes. The measured radial distributions were not used because they refer to hardwall modes only; when the sound field enters the lined section, considerable scattering is expected among the various radial orders.

The results of this study are shown in Fig. 16. The lining design details are given in Fig. 16a, while Fig. 16b shows the attenuation for the two linings under each of the two assumptions. For the observed ($m = -13$) modal structure, the optimized lining has a predicted average attenuation of 23 dB, while the other lining has 20 dB. The difference, 3 dB in this case, is the lining advantage due to better knowledge of the modal structure. In this particular case, the advantage is relatively small (only 15%) because the $m = -13$ mode is close to a "typical" mode in this duct. If the true noise field were dominated by a more unusual mode, the difference would be more dramatic. To take an extreme example, the plane-wave mode would have about a 0.2-dB attenuation with the equal amplitude lining design but could have a 1.0-dB attenuation

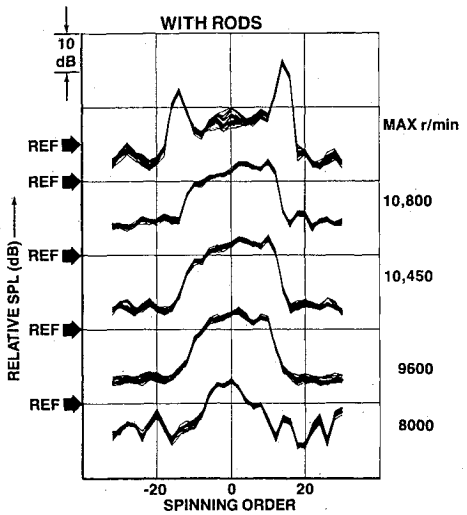

Fig. 13 SPL vs spinning order at one-half blade passage frequency.

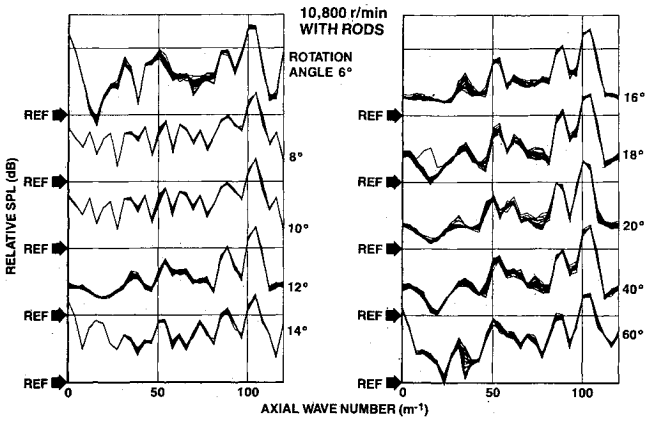

Fig. 14 SPL vs axial wavenumber at blade passage frequency (various duct rotation angles).

DUCT LENGTH	9.56 in (0.243 m)
DIAMETER	21 in (0.533 m)
MEAN FLOW MACH NO.	0.2
BOUNDARY LAYER THICKNESS	0.014 in (.000356 m)
AIR DENSITY	0.0755 lbm/ft³ (1.21 kg/m³)
AIR TEMPERATURE	21°C

a) Duct parameters

b) Lining design

r/min	RELATIVE LEVEL IN VARIOUS MODES (dB) (-13,0)	(-13,1)	(-13,2)	(22,0)
8000	105.5	-	-	-
9600	107.5	97.5	-	-
10,450	106.5	100.0	92.5	96-99

c) Modal structure

Fig. 15 Parameters used for lining design.

	EQUAL AMPLITUDE	m = 13 ONLY
OUTER FACE SHEET (R/ρc)	2.17	1.90
OUTER CORE DEPTH (in)	0.35	0.35
INTERIOR SHEET (R/ρc)	1.52	2.72
INNER CORE DEPTH (in)	0.35	0.25

a) Lining designs

	EQUAL AMPLITUDE LINING DESIGN	m = 13 LINING DESIGN
WITH EQUAL AMPLITUDES		
8000 r/min	6.24	6.01
9600 r/min	5.99	5.78
10,450 r/min	5.78	5.63
AVERAGE	6.00	5.80
WITH m = 13 ONLY		
8000 r/min	30.54	36.77
9600 r/min	19.71	22.27
10,450 r/min	17.46	21.04
AVERAGE	20.07	23.31

b) Lining attenuation (dB)

Fig. 16 Final lining design and performance.

from an optimized lining—a 400% improvement. Thus, the advantage to be gained in lining design depends strongly on the actual modal structure and is greater when the field is dominated by hard-to-attenuate modes.

Concluding Remarks

This mode measurement technique was developed for the dual purposes of studying turbomachinery noise mechanisms and designing optimum linings. It has proved reliable and robust; in particular, the analysis is tolerant of calibration errors and unsteady rotor speeds. The system has been successfully used to identify quantitatively the source mechanisms in full-scale engine inlets. Studies indicate that more efficient linings can be designed using information from this system, although the magnitude of the improvement depends on the particular modal structure.

Acknowledgments

The experimental portion of this work was a joint project with the NASA Langley Research Center, which provided the test facility and engine. Special thanks are due to Jim Schoenster and Bob Golub of NASA. The data acquisition system owes its existence to the dedicated efforts of Ron Zwilling and Howard Burch of Boeing.

References

[1]Mungur, P. and Gladwell, G. M. L., "Acoustic Wave Propagation in a Sheared Fluid Contained in a Duct," *Journal of Sound and Vibration*, Vol. 9, Jan. 1969, pp. 28-48.

[2]Pickett, G. F., Sofrin, T. G., and Wells, R. A., "Method of Fan Sound Mode Structure Determination—Final Report," NASA CR-135293, Aug. 1977.

[3]Zandbergen, T., Laan, J. N., and Zeemans, H. J., "In-Flight Acoustic Measurements in the Engine Intake of a Fokker F28 Aircraft," AIAA Paper 83-0677, April 1983.

[4]Rice, E. J., "Acoustic Liner Optimum Impedance for the Spinning Modes with Mode Cut-Off Ratio as the Design Criterion," AIAA Paper 76-516, July 1976.

[5]Bucker, H. P., "Cross-Sensor Beam Forming With a Sparse Line Array," *Journal of the Acoustical Society of America*, Vol. 61, Feb. 1977, pp. 494-498.

[6]Schoenster, J. A., "Fluctuating Pressure Measurements on the Fan Blades of a Turbofan Engine During Ground and Flight Tests," AIAA Paper 83-0679, April 1983.

[7]Tyler, J. M. and Sofrin, T. G., "Axial Flow Compressor Noise Studies," *Transactions of the SAE*, Vol. 70, 1962, p. 309.

[8]Lester, H. C., Preisser, J. S., and Parrott, T. L., "The Design and Flight Test of an Engine Bulk Acoustic Liner," AIAA Paper 83-0781, April 1983.